Eur. Phys. J. B **40**, 445–452 (2004)
DOI: 10.1140/epjb/e2004-00248-0

THE EUROPEAN PHYSICAL JOURNAL B

High-field interlayer tunnelling transport in layered cuprates: Uncovering the pseudogap state

L. Krusin-Elbaum[1,a] and T. Shibauchi[2]

[1] IBM T.J. Watson Research Center, Yorktown Heights, New York 10598, USA
[2] Department of Electronic Science and Engineering, Kyoto University, Kyoto 615-8510, Japan

Received 2 February 2004
Published online 10 August 2004 –

Abstract. In high temperature (high T_c) cuprate superconductors the gap in the electronic density of states is not fully filled at T_c; it evolves into a partial (pseudo)gap that survives way beyond T_c, challenging the conventional views. We have investigated the pseudogap phenomenon in the field-temperature $(H - T)$ diagram of $Bi_2Sr_2CaCu_2O_{8+y}$ over a wide range of hole doping $(0.10 \leq p \leq 0.225)$. Using interlayer tunneling transport in magnetic fields up to 60 T to probe the density-of states (DOS) depletion at low excitation energies we mapped the pseudogap closing field H_{pg}. We found that H_{pg} and the pseudogap onset temperature $T^\star$ are related via a Zeeman relation $g\mu_B H_{pg} \approx k_B T^\star$, irrespective of whether the magnetic field is applied along the c-axis or parallel to CuO_2 planes. In contrast to large anisotropy of the superconducting state, the field anisotropy of H_{pg} is due solely to the g-factor. Our findings indicate that the pseudogap is of singlet-spin origin, consistent with models based on doped Mott insulator.

PACS. 74.25.Dw Superconductivity phase diagrams – 74.25.Fy Transport properties (electric and thermal conductivity, thermoelectric effects, etc.) – 74.72.Hs Bi-based cuprates

1 Introduction

The physics of high transition temperature superconductivity in copper oxides is still one of the outstanding unsolved problems in condensed matter physics. Superconductivity in cuprates arises from doping the charge carriers into a Mott insulating parent compound, with the ground state controlled by competing orders [1]. In Mott insulators, being half-filled (with one hole per Cu), the antiferromagnetism and insulating behavior are a consequence of strong on-site Coulomb repulsion between the copper d electrons. And it is generally thought that these correlated d electrons are essential to the high T_c [2]. A distinguishing feature of doped Mott insulators is a strong sensitivity of their ground state to doping, and this is reflected in the putative phase diagram sketched in Figure 1. The antiferromagnetic region at low doping (for both electron and hole-doped materials [3,4]) disappears with increasing doping, being eventually replaced by the superconducting 'dome' region, bounded by the T_c that (at least in the hole doped cuprates) is phenomenologically found to follow a parabolic doping dependence [5] $T_c/T_c^{\max} = 1 - 82.6(p - 0.16)^2$, with p denoting the doping level. In-between, spin correlations may be felt in a variety of ways. There may be mesoscopically inhomogeneous phases (stripes) [6] and then there is this ubiquitous pseudogap phenomenon, which manifests itself as a depletion of the quasiparticle density of states (DOS) below a characteristic temperature $T^\star$, and is particularly prominent in the low doping (underdoped) side of the superconducting dome. By a way of contrast, on the high doping (overdoped) side cuprates are deemed conventional, and as such are expected to display behaviors of conventional (Fermi-liquid) metals.

However, uncertainties are many. This normal state pseudogap [7,8] is the most salient and fiercely debated feature in the phase diagram of cuprate superconductors, but it's link to the superconductivity with high T_c is still unclear. The central issue is whether the pseudogap originates from spin or charge degrees of freedom and, in particular, whether it derives from some sort of precursor of Cooper pairing that acquires the superconducting coherence at T_c. Experimentally, the situation appears deeply conflicted. On the one hand, photoemission [9] and surface tunnelling spectroscopy [10,11] show the pseudogap continuously evolving into a superconducting gap below T_c [12]. The reports of anomalous and large Nernst effect in the normal state [13] led to claims of vortex-like excitations surviving up to temperatures close to $T^\star$. On the other hand, intrinsic tunneling measurements revealed a double gap structure [14,15], indicating the pseudogap distinct even below T_c. With very different magnetic field sensitivities [16], the two gap features have been viewed

[a] e-mail: krusin@us.ibm.com

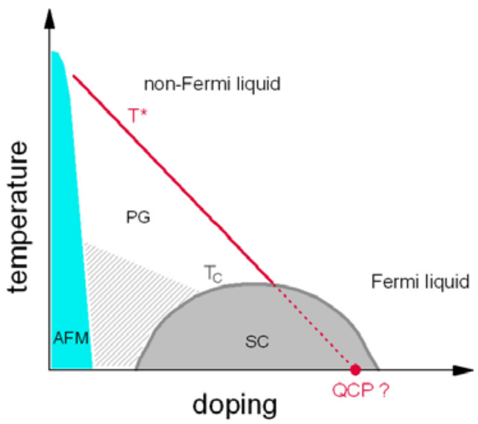

Fig. 1. A sketch of the generalized phase diagram of hole-doped cuprates showing the antiferromagnetic (AFM) insulator regime at low doping, the superconducting (SC) 'dome', and the vast pseudogap region (PG) below the characteristic temperature $T^\star$. How and where the $T^\star$ line reaches the zero value is still unknown.

by some as being unrelated [17]. This view is strongly argued in the, so called, 'competitor' scenarios [18,19] which require the pseudogap closed in a phase transition at the quantum critical point, turning the cuprate pseudogapless on the overdoped side of the dome, but not far from the optimal doping $p = 0.16$.

Recently we have shown that in magnetic fields along the c-axis, the field H_{pg} that closes the pseudogap Δ_{pg} relates to $T^\star$ via a simple Zeeman relation [20], suggesting that Δ_{pg} is controlled by the spin- rather than orbital degrees of freedom. However, several 'precursor superconductivity' scenarios, for example, those based on BCS-Bose Einstein crossover [21] or on intermediate coupling [22] models, argue that Zeeman scaling is compatible with the superconducting origin of the pseudogap.

Here we will discuss our experiments probing the pseudogap state at ultrahigh magnetic fields using interlayer (c-axis) tunnelling transport as a probe. Our task here will be to draw a map of the H-T-p diagram of the pseudogap state, to test the field anisotropy of H_{pg} and compare it with the anisotropy of the superconducting state, to access the role of fluctuations in the high-field/low-temperature regime, and to search for the presence of a quantum critical point (QCP). We find that the pseudogap closing field obeys a Zeeman scaling relation $g\mu_B H_{pg} \approx k_B T^\star$ regardless of the field orientation. And while in the superconducting state anisotropy *is* large, $H_{pg}(T)$ displays only a small anisotropy of the the (spectroscopic splitting) Landé g-factor of the Cu^{2+} ions. Given the scales for H_{pg} and $T^\star$, the Zeeman splitting for the spin degrees of freedom appears not in correspondence with pair-breaking via a conventional paramagnetic (Pauli) effect [23]. The observed Zeeman relation and the absence of orbital frustration naturally points to a singlet spin-correlation gap closed with a triplet spin excitation at H_{pg}. The pseudogap is clearly present up to a very high doping level and no evidence for the quantum critical point (QCP) is found up to $p = 0.225$.

2 Interlayer tunnelling resistivity at high magnetic fields as a probe of the pseudogap

Among various techniques that quantify DOS, the measurements of the interlayer tunnelling resistivity ρ_c are uniquely suited for exploring the highest magnetic field range available mostly in a pulsed mode. In materials, such as $Bi_2Sr_2CaCu_2O_{8+y}$ (Bi-2212), that are strongly anisotropic and where interlayer coupling between CuO_2 layers is sufficiently weak, the c-axis transport directly measures Cooper pair or quasiparticle tunneling in both normal and superconducting states [24], providing *bulk* information about the quasiparticle DOS at the Fermi energy. Indeed, in the case of Bi-2212, $\rho_c(T)$ fully corresponds to the measured differential tunnelling resistivity $dV/dI(T)$ at zero bias measured in the mesoscopic mesa-shaped structures carved out of single crystals, comprising several CuO_2 planes separated by ~ 15 Å thin intrinsic tunnelling barriers [14]. ρ_c is particularly sensitive to the onset of the pseudogap formation, since the DOS depletion is largest at the Fermi energy. Moreover, ρ_c is informed by the vicinity of the $(\pi, 0)$ points (the so called 'hot spots') on the anisotropic Fermi surface [25,26], where the pseudogap first opens up [9]. (This is in contrast to the in-plane resistivity ρ_{ab} mainly determined by carriers with momenta parallel to the (π, π) directions [25].)

One important consequence of the pseudogap is the temperature dependence of (anisotropic) normal state resistivity. The in-plane resistivity ρ_{ab} is metallic ($d\rho_{ab}(T)/dT > 0$) and T-linear at high temperatures (above $T^\star$) but is believed to decrease on cooling faster near the opening of the pseudogap [27]. However, ρ_c turns from metallic to semiconductinglike ($d\rho_c(T)/dT < 0$) at $T^\star$ above onset of the deviation from the T-linear behavior in ρ_{ab} [28,29]. Tunnelling spectroscopy data [30] indicate that the 'pseudogap temperature' – defined as the temperature at which the conductance dI/dV develops a dip at zero-bias – corresponds to $T^\star$ from the c-axis transport. Moreover, the pseudogap phase boundaries obtained from the ρ_c and from the static susceptibility measurements appear to coincide [28].

To elucidate the field and temperature dependence of the pseudogap over a wide doping range, we carefully adjusted hole concentration p spanning both underdoped and overdoped regimes in Bi-2212 crystals grown by the floating-zone method. The doping level was controlled by annealing in O_2 or N_2 at the appropriate pressures. $\rho_c(H)$ was measured using a 33 T dc magnet and a 60 T long (2 s and 60 ms) pulse systems at the National High Magnetic Field Laboratory (NHMFL). In the pulse magnets we used a lock-in technique at 100 kHz. Negligible eddy-current heating was verified by the consistency of the data taken with successive pulses to different target fields.

2.1 Temperature dependence of ρ_c

The temperature dependence of the c-axis resistivity ρ_c for a Bi-2212 crystal ($p \simeq 0.2$) with $T_c = 78$ K is shown in Figure 2a. On cooling, at a temperature above T_c the zero-field $\rho_c(T)$ develops an upward deviation from the metallic dependence at the pseudogap temperature $T^\star$ [28,29]. At this temperature the magnetoresistance (MR) changes sign – the negative MR is due to the field suppression of the pseudogap, i.e. a recovery of the depleted DOS by the magnetic field. The semiconductinglike upturn at $H = 0$ is not so apparent if the doping level is sufficiently high. For example, an overdoped (OD) crystal in Figure 3 with $T_c = 60$ K ($p = 0.225$) is so overdoped that the zero-field $\rho_c(T)$ is metallic nearly all the way down to T_c. However, even a moderate magnetic field (~ 10 T) along the c direction exposes the upturn in $\rho_c(T)$ before it plunges to zero in the dissipationless state below T_c. Further increases in field affects the pseudogap itself, namely the upturn is suppressed and the metallic regime is extended to lower temperatures. In overdoped samples, $T^\star$ can be very close to T_c, or may be below T_c, see reference [14].

In the OD crystal with $T_c = 67$ K ($p = 0.22$) a magnetic field of ~ 60 T downshifts the semiconducting upturn in $\rho_c(T)$ and the associated $T^\star$ by about 20 K [20], see Figure 2b. In other words, at this doping level, the 60 T field at ~ 100 K closes the pseudogap. To track the pseudogap closing field at lower temperatures and higher fields, we consider the excess resistivity $\Delta\rho_c$ due to the pseudogap. $\Delta\rho_c$ is obtained by subtracting the T-linear contribution [20]. The T-linear behavior of ρ_c is observed over a large temperature range above $T^\star$ and there is no indication of a different temperature dependence when the 'true' ungapped normal state is restored.

2.2 Field dependence of ρ_c; Josephson and quasiparticle c-axis tunnelling in a layered cuprate

In the superconducting state, $\rho_c(H)$ becomes finite above the irreversibility field H_{irr} ($\equiv$ zero resistivity field $H_{0\rho}$ in Fig. 4). This signals the entry into a vortex liquid state. A characteristic peak is observed at a higher field H_{sc}. This peak arises from a competition between two parallel tunnelling conduction channels [24]: σ_J of Cooper pairs (Josephson tunnelling that decreases with increasing field) and σ_q of quasiparticles (dominating at high fields). The entire c-axis conductivity σ_c can be written as:

$$\sigma_c = \underbrace{\sigma_{J0}\exp\left[\frac{U(H)}{T}\right]}_{\sigma_J} + \underbrace{\sigma_{q0}\left(1+\frac{H}{H_\Delta}\right)}_{\sigma_q}, \tag{1}$$

with σ_J controlled by the thermally activated diffusive drift of pancake vortices hopping over the energy barriers $U(H)$ in the CuO_2 planes [31]. Here, σ_{J0} and σ_{q0} are the $T = 0$ values of Josephson and (nodal) quasiparticle tunnelling conductivities, and $H_\Delta = \Phi_0\Delta^2/\hbar^2 v_F^2$, where Δ is the gap in the quasiparticle spectrum [24]. Note that in the BCS theory H_Δ corresponds to the conventional

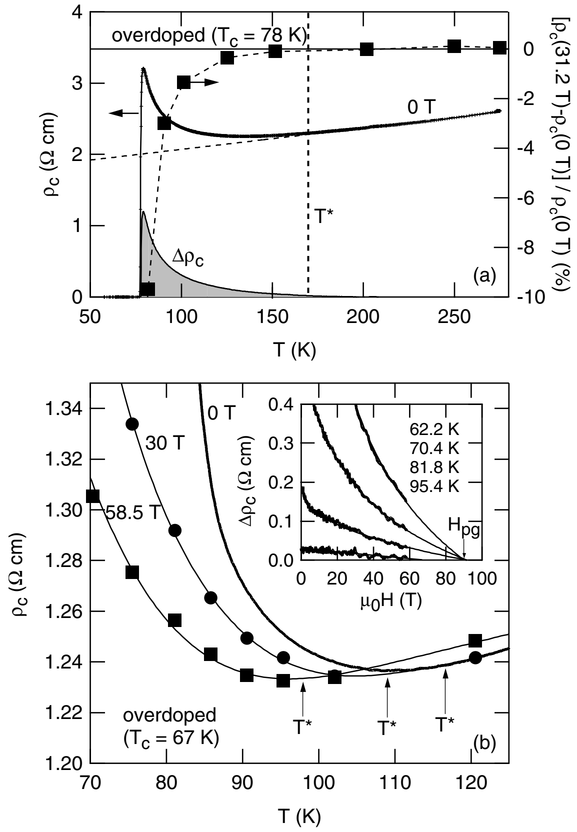

Fig. 2. Determination of the pseudogap temperature $T^\star$ and the pseudogap closing field H_{pg} from $\rho_c(T,H)$ in overdoped Bi-2212. (a) $\rho_c(T)$ deviates from metallic T-linear dependence at the same temperature where negative MR $= [\rho_c(H) - \rho_c(0)]/\rho_c(0)$ disappears, identified as pseudogap temperature $T^\star$. (b) For $T_c = 67$ K, $T^\star$ is shifted by ~ 20 K by a 58.5 T field. Inset: The excess quasiparticle resistivity $\Delta\rho_c(H)$ (above H_{sc}) is fitted to a power-law field dependence $[\Delta\rho_c(H) - \Delta\rho_c(0)] \propto H^\alpha$.

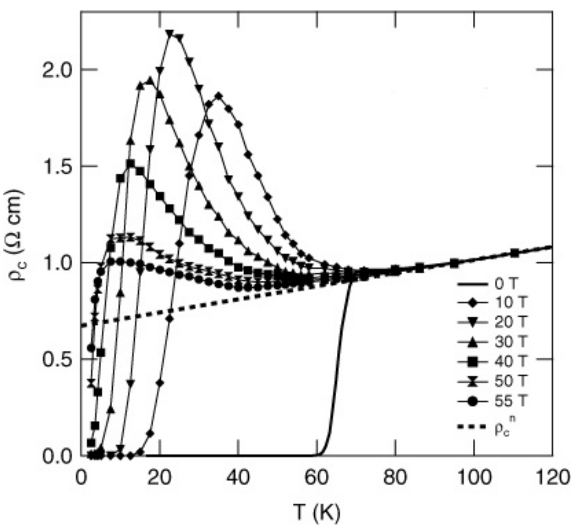

Fig. 3. c-axis resistivity vs. temperature in overdoped Bi-2212 (with the hole doping level $p = 0.225$) up to 55 T $\| c$. The normal state resistivity $\rho_c^n(T)$ is shown as dashed line. Here the pseudogap temperature $T^\star \sim 100$ K.

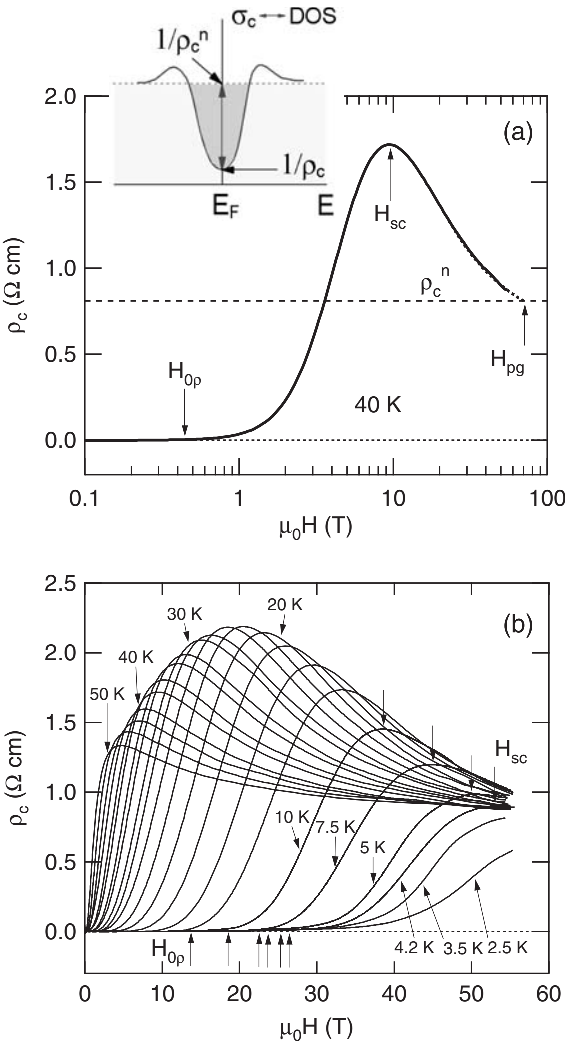

Fig. 4. (a) $\rho_c(H)$ is marked by three characteristic fields: (zero-resistivity) $H_{0\rho} \equiv H_{irr}$, H_{sc}, and H_{pg}. The ungapped state value ρ_c^n (dashed line) is reached at the pseudogap closing field H_{pg}. The data are for an overdoped crystal with $T_c = 60$ K. Inset: ρ_c is the inverse of the interlayer tunneling conductivity σ_c near Fermi energy $E = E_F$. (b) The peak field at H_{sc}, and the irreversibility field H_{irr} both strongly upshift on cooling. The data shown here are for $H \parallel c$.

$H_{c2} \sim \Phi_0/2\pi\xi^2$. The remarkable H-linear behavior of σ_q at high fields is directly seen from our measurements of $I-V$s in the Bi-2212 mesas, where we measured quasiparticle conductivity up to 33 T (see Fig. 5) after suppressing the Josephson contribution with current.

Taking the derivative of equation (1) with respect to H and recalling that $U(H) = U_0 \ln\frac{H_0}{H}$ for a 2D vortex lattice [32], we obtain the expression for the field H_{sc} where the maximum in ρ_c (minimum in σ_c) will occur,

$$H_{sc}(T) \cong H_0 \left[\frac{\sigma_{q0}}{\sigma_{J0}}\frac{T}{U_0}\frac{H_0}{H_\Delta}\right]^{-\frac{T}{U_0}}. \qquad (2)$$

Indeed, this high field $H_{sc}(T \to 0)$ can hardly be distinguished from a T-exponential consistently observed in

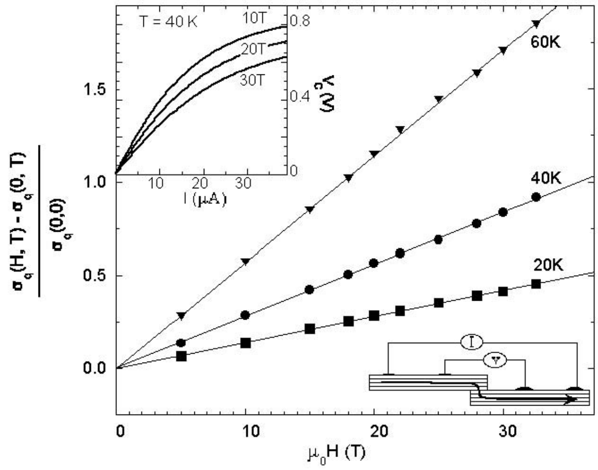

Fig. 5. Normalized quasiparticle c-axis conductivity as a function of $H \parallel c$ obtained from the $I-V$ curves (top inset) measured on the mesa shaped crystals of Bi-2212 (sketched).

the entire doping range. At H_{sc}, the quasiparticle and the Josephson tunnelling currents are comparable. Above the peak at $H_{sc}(T)$, the magnetoresistance is negative and follows a power-law (see legend of Fig. 2) until the pseudogap is quenched at H_{pg} when $\rho_c(H)$ reaches the ungapped normal state resistivity ρ_c^n (Figs. 2–5).

3 The role of spins in the formation of the pseudogap

3.1 Closing the pseudogap by Zeeman splitting

At the closing of the pseudogap $\Delta\rho_c \to 0$ and we determine the pseudogap closing field $H_{pg}(T)$ beyond 60 T by a fit to the power-law field dependence [24] of $\Delta\rho_c(H)$ at different temperatures. This illustrated in the inset of Figure 2b. Figure 6 shows the doping dependence of the pseudogap closing field $H_{pg}(p)$ and $T^\star$. H_{pg} and $T^\star$ obtained independently in the same crystals in the OD regime, scale through a strightforward Zeeman energy relation $g\mu_B H_{pg} \approx k_B T^\star$ with $g = 2.0$. Here μ_B is the Bohr magneton, and k_B is the Boltzmann constant. This implies that magnetic field couples to the pseudogap by the Zeeman energy of the spin degrees of freedom. It all indicates a predominant role of spins over the orbital effects in the formation of the pseudogap. Our evaluation of H_{pg} gives a consistent and physically sensible picture, since at low temperatures $H_{pg}(T)$ is flat in underdoped samples as well, and $H_{pg}(p)$ is a smooth continuation from the overdoped side. We surmise that the Zeeman scaling found in the OD samples holds in the entire doping range of this study.

Notably, the doping dependencies of the peak field $H_{sc}(p)$ and $H_{pg}(p)$ are drastically different. At H_{sc} we have still a small but finite Josephson current which is a measure of the superconducting coherence. This naturally accounts for a parabolic doping dependence of $H_{sc}(p)$

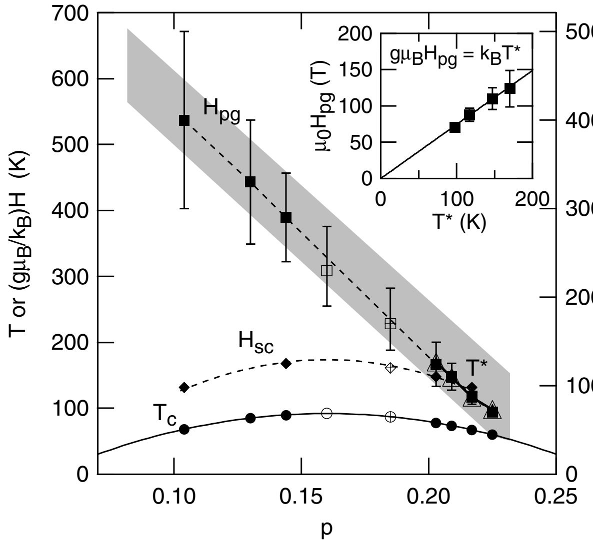

Fig. 6. Doping dependence of low-temperature H_{pg} (squares) and H_{sc} (diamonds) in Bi-2212 together with $T^\star$ (open triangles) and T_c (circles). The hole concentration p was obtained from the empirical formula $T_c/T_c^{max} = 1 - 82.6(p-0.16)^2$ [17] with $T_c^{max} = 92$ K. The shaded band covers $T^\star(p)$ in cuprates determined by several techniques (taken from Ref. [7]). Inset: For $H\|c$ the pseudogap closing field H_{pg} and $T^\star$ follow a simple Zeeman scale $g\mu_B H_{pg}^{\|c} \approx k_B T^\star$ with $g = 2.0$ down to the hole doping level $p = 0.225$.

similar to that of $T_c(p)$ where the superconducting coherence is established at zero field.

3.2 Anisotropy of the pseudogap state

Conventionally, the upper critical field $H_{c2} \cong \Phi_0/2\pi\xi^2$ is determined not directly by the gap, but by the coherence length ξ (the size of the Copper pair). The orbital motion of the Cooper pairs with increasing field eventually leads to diamagnetic pair breaking, restoring the normal state. Ginzburg-Landau description of anisotropic 3D superconductor gives $H_{c2}^{ab} = \Phi_0/2\pi\xi_{ab}\xi_c$ (for the field in the ab-plane) and $H_{c2}^{c} = \Phi_0/2\pi\xi_{ab}^2$ (for the field along the c-axis), where Φ_0 is the flux quantum [33]. In cuprates, the field anisotropy $\gamma = H_{c2}^{ab}/H_{c2}^{c} = \xi_{ab}/\xi_c$ is large [34], since the coherence length ξ_c along the c-axis (~ 2 Å) is much shorter than the in-plane ξ_{ab} (~ 20 Å). In the 'precursor' view, one would similarly expect an orbital frustration of preformed pairs at the pseudogap closing field.

Figure 7 shows the peak at H_{sc} upshifting with decreasing temperature at a rate much faster for $H\|ab$ than for $H\|c$. This is understood because H_{sc} is a 'practical' measure – a reliable lower bound [24] on H_{c2}. The temperature dependence of H_{sc} in Figure 8a shows that not only the initial slope for the two field alignments is very different, namely, $dH_{sc}^{ab}/dT|_{T_c} = -3$ T/K is much larger than $dH_{sc}^{c}/dT|_{T_c} = -0.27$ T/K, but also the overall curvature changes from concave to convex when the field is rotated from the out- to in-plane. This is reflected in

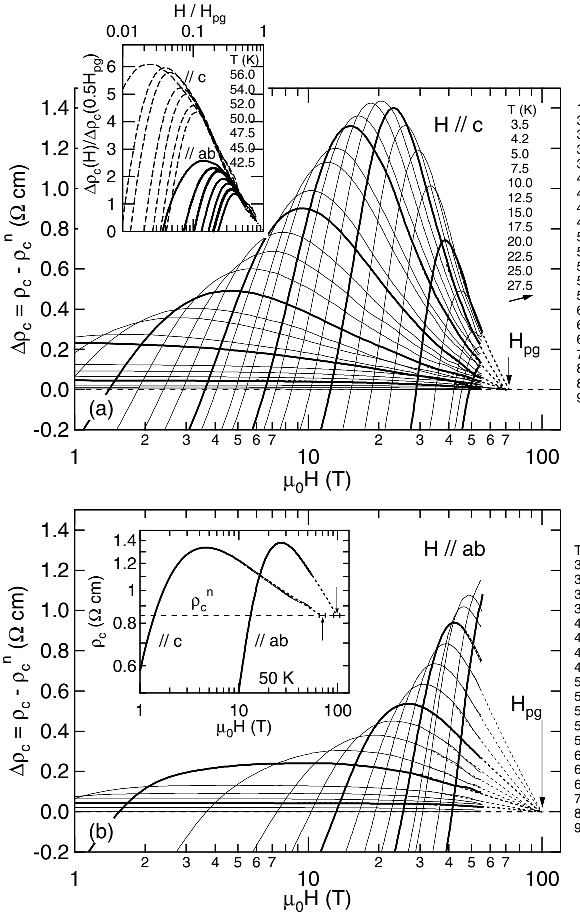

Fig. 7. Excess c-axis resistivity $\Delta\rho_c = \rho_c - \rho_c^n$ vs. field [after subtracting the ungapped normal state resistivity $\rho_c^n(T)$] for (a) $H\|c$ and (b) $H\|ab$. All curves are labelled by temperatures. $\Delta\rho_c$ above the resistivity maximum at H_{sc} follows a power-law. At each temperature the pseudogap is extinguished at a closing field $H_{pg}(T)$ when $\Delta\rho_c(H) \to 0$. Top inset: The high-field collapse on the same scaling curve of $\Delta\rho_c(H)$ plotted *vs* H/H_{pg} for many temperatures enables us to independently track $H_{pg}(T)$ for $H\|c$ and $\|ab$. Above $0.5H_{pg}$ the Josephson current contribution is negligible. Bottom inset illustrates a power-law fit at $T = 50$ K. Bars indicate the errors associated with the fits.

the strong temperature dependence of the anisotropy ratio $\gamma_{sc} = H_{sc}^{ab}/H_{sc}^{c}$, which is ~ 12 close to 55 K but decreases by a factor of 3 near $0.5T_c$. Indeed, in the quasi-2D regime at high fields (when $\xi_c(T)$ becomes smaller than the interlayer distance $d \sim 15$ Å), the temperature dependent H_{c2} anisotropy below T_c derived for weakly coupled superconducting layers stacked in the c-direction is $\gamma \propto 1/\sqrt{1-T/T_c}$ [35]. This T-dependence is well followed by γ_{sc} (Fig. 8b), with the $T \to 0$ limit in good correspondence with the ($\sim 3-4$) anisotropy reduction with doping. The irreversibility anisotropy (also T-dependent) is even larger; $H_{irr}^{ab}/H_{irr}^{c} \approx 20-30$ near 30 K, as shown in Figures 8c and 8d.

To quantify the anisotropy of the pseudogapped state [36] we used the identical procedure for $H\|c$ and

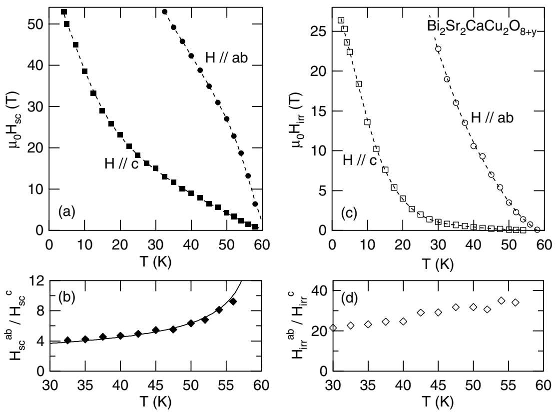

Fig. 8. Anisotropy of the characteristic fields in the superconducting state. (a) The peak field $H_{sc}(T)$ and (c) the irreversibility field $H_{irr}(T)$ for $H \| c$ and $H \| ab$. H_{irr} was determined using a $\rho_c = 0.01\rho_c^n$ criterion, consistent with our experimental resolution. Large anisotropy of H_{sc} and H_{irr} is seen in the ratios for the two field configurations in (b) and (d) respectively.

$H \| ab$ to evaluate the excess quasiparticle resistivity $\Delta\rho_c$. Figure 7 shows that for the in-plane applied field $\rho_c(H)$ has to be extrapolated somewhat further to reach the ungapped normal state value than for $H \| c$ ('weak' anisotropy in the normal state up to 14 T was reported in [37,38]). The values of $H_{pg}(T)$ can be independently tracked from the high-field scaling behavior of $\Delta\rho_c$ for $H \to H_{pg}$ shown in Figure 7 (top inset).

The obtained pseudogap closing field $H_{pg}(T)$ for the two orthogonal field orientations is plotted in the $H - T$ diagram in Figure 9. In contrast to H_{sc} and H_{irr}, $H_{pg}(T)$ is T-independent below $\sim 0.8T^\star$. The 'flatness' of $H_{pg}(T)$ below roughly $0.8T^\star$ has been consistently observed for $H \| c$ at *all* doping levels ($p = 0.1 - 0.225$). Here we see that this flatness is a unique thumbprint of the pseudogap closing field irrespective of the field direction. The consequence of this is twofold. One, it leaves no doubt that the anisotropy $\gamma_{pg} = H_{pg}^{\|ab}/H_{pg}^{\|c}$ is temperature-independent from $\sim$ 80 K down to at least $0.4T^\star$. Moreover, as the inset shows, $\gamma_{pg} \approx 1.35 \pm 0.1$ all the way up to $\sim T^\star$. Two, since it robustly projects to the zero-temperature values of $H_{pg}(T)$ (≈ 71 T for $H \| c$ and ≈ 96 T for $H \| ab$), this directly translates into a Zeeman scaling relation $g^{\|c}\mu_B H_{pg}^{\|c}(T = 0) = g^{\|ab}\mu_B H_{pg}^{\|ab}(T = 0) \approx k_B T^\star(H = 0)$, with the g-factor anisotropy $g^{\|c}/g^{\|ab} \equiv \gamma_{pg}$, indicating the Δ_{pg} closing to be a 'massless' process. Indeed, independent measurements [28] of uniform spin susceptibilities $\chi_{ab}(H \| ab)$ and $\chi_c(H \| c)$ in Bi-2212 give a constant $\chi_c/\chi_{ab} = (g^{\|c}/g^{\|ab})^2 \approx 1.6$, in complete correspondence with the pseudogap anisotropy γ_{pg}.

4 Huge quantum fluctuations at high magnetic fields

One important question raised about the strongly OD regime concerns the role of fluctuations. There the difference between the $T^\star$ and T_c may not be well discernible, because thermal (classical) fluctuations are very large [33]. One way to address this issue is to consider quantum fluctuations at ultrahigh fields. Evaluating the significance of quantum fluctuations is a harder task, and estimating (very high) H_{c2} in the cuprates has been a subject of much controversy [33], not surprisingly aggravated by the pseudogap below $T^\star$. We have found [39] that in strongly overdoped Bi-2212, as $T \to 0$ the magnetic field that closes the pseudogap and the upper critical field H_{c2} coincide, uniquely defining the upper limit on the vortex state. By mapping the upper and lower bounds on the molten vortex state, we have found the gapped quantum fluctuation regime stretches from $\sim$ 30 to 70 T. This exceeds by far the conventional estimates, pointing to the anomalous gapped nature of the strongly overdoped regime.

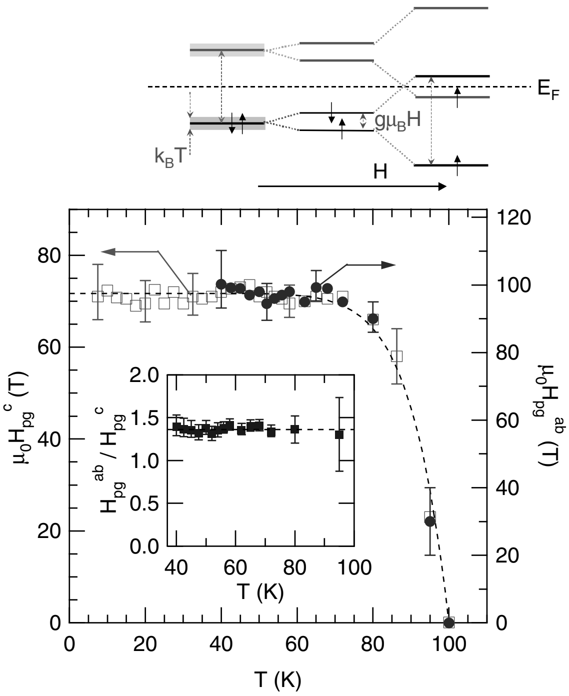

Fig. 9. The pseudogap closing field $H_{pg}(T)$ for $H \parallel c$ (left hand side) and $H \parallel ab$ (right hand side) in Bi-2212 with $p = 0.225$. The error bars indicate the uncertainties in the power-law fits. The ratio $H_{pg}^{\|ab}(T)/H_{pg}^{\|c}(T) \approx 1.35$ is temperature independent (inset) and corresponds to the anisotropy of the g-factor. This points to the separate spin- and charge-correlation channels with the spin-gap closed at H_{pg} by a triplet excitation, as sketched in the outset.

The observed ease of vortex displacements by zero-point vibrations naturally points to a modified structure of the vortex core. The pseudogapped core has been experimentally demonstrated by scanning tunnelling spectroscopy [10]. And from phenomenological considerations, the observed reduction in the effective viscosity η [40] (implying a higher vortex velocity) points to a reduced number of carriers available for pushing the current through the core, consistent with the pseudogaped cores.

5 What about a quantum critical point?

The $T - p - H$ diagram for a strongly overdoped Bi-2212 with $p = 0.225$ is compiled in Figure 10. Here we focus on the low temperature regime. In a view where the deduced QCP is near $p = 0.19$ [17] the difference between T_c and $T^\star$ (double-ended arrow) beyond the QCP may come from thermal fluctuations. However, the unconventionally large dissipative gapped state we observe at high fields as $T \to 0$ may suggest the pseudogap in the quantum limit far on the overdoped side. This picture is consistent with the upturn in the $\rho_c(T)$ recovered in a moderate magnetic field, and the smooth continuity of $H_{pg}(p)$ from the UD side [20] with its 'flat' low-temperature behavior at *all* doping levels. Therefore, we conclude that there is no experimental support from the ρ_c measurements for the quantum critical point up to $p = 0.225$.

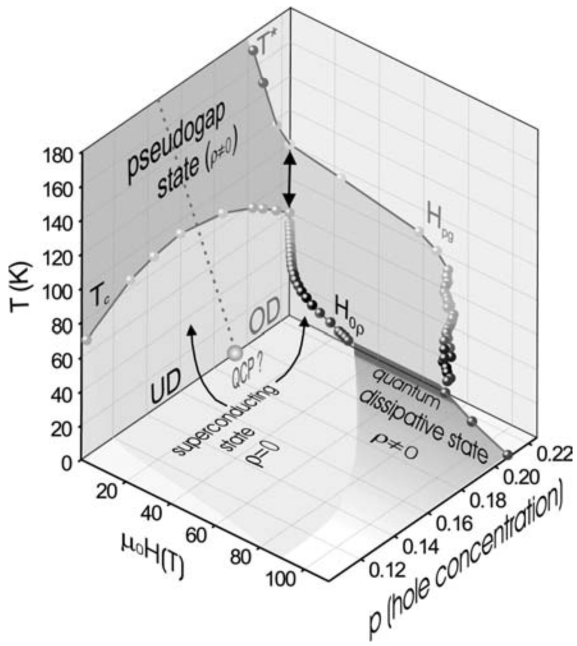

Fig. 10. Temperature-field-doping diagram of Bi-2212 highlighting the overdoped region up to $p = 0.225$ near T_c and near $T = 0$. The unconventionally large dissipative gapped state (DGS) in the $T = 0$ limit is consistent with the pseudogapped vortex cores in the overdoped regime.

6 Separated spin and charge degrees of freedom

Let us now consider the field scales corresponding to the pseudogap energy $T^\star$. Recently, Wang et al. [41] measured thermal (in-plane) Nernst transport in Bi-2212 and from that deduced values of an orbital limiting 'upper critical field' H_{c2}^N, past which the charge pairing amplitude should vanish. H_{c2}^N was found to decrease steeply with increased doping, implying that the Cooper pairing potential and the superfluid density follow opposite trends versus charge doping. This led Wang et al. to an interpretation [41] of the role of phase fluctuations in the low doping region. Central to understanding this observation is how the Nernst-derived H_{c2}^N relates to the gap $T^\star$ observed by angle-resolved photoemission (ARPES) [9,26,42], as well as by the intrinsic tunnelling [14] spectroscopies: pairing correlations are quenched through localization in a magnetic field H once the magnetic length a_0 drops below the pair correlation length $\xi^\star = \hbar v_F/\alpha T^\star$. Here, v_F is the Fermi velocity and α is a numerical of order unity. Indeed, the Nernst-derived magnetic field appears to well match this condition [41] and hence qualifies as an orbital limiting (or critical) magnetic field H_{c2}^N; as such it scales *quadratically* in T^*, $\mu_B H_{c2}^N \sim T^{*2}/mv_F^2$.

Remarkably, a 'critical' magnetic field H_{pg} derived from our c-axis interlayer tunnelling transport measurements is much higher than H_{c2}^N . Given the equivalence of the limiting fields H_{pg} and H_{c2}^N to the same pseudogap energy scale $T^\star$ but via different routes, 'orbital' for H_{c2}^N and 'Zeeman' for H_{pg}, we can simply derive how the two fields relate (as a function of doping p),

$$H_{c2}^N(p) = H_{c2}^\star(p) \equiv \alpha^2 \frac{\mu_B H_{pg}(p)}{mv_F^2} H_{pg}(p). \qquad (3)$$

Note that equation (3) rests only on pairing (and the uncertainty principle) combined with the definitions of the Zeeman energy and the magnetic length.

With the Fermi velocity v_F insensitive to doping [42], equation (3) predicts a simple quadratic relation $H_{c2}^N(p) \propto H_{pg}^2(p)$. Comparing $H_{c2}^N(T \cong 0)$ and $H_{c2}^\star(0)$ by using most recently measured values for the Fermi velocity [43] $v_F \simeq 2$ eVÅ and choosing $\alpha \approx 0.6$, we obtain a proper collapse of the data in the low doping (underdoped) regime $p < 0.16$ [44]. Close to optimal doping, the scaled and the measured orbital fields part their ways: $H_{c2}^\star$ enters the superconducting 'dome' while the H_{c2}^N follows its edge, pointing to a remarkable distinction between the low- and the high-doping sides [42].

Having the two critical fields H_{c2}^N and H_{pg} related to a single energy scale T^*, the question arises how one could dispose of the same correlation energy twice: via the orbital route at H_{c2}^N and then again via the Zeeman effect at $H_{pg} \gg H_{c2}^N$. This 'double jeopardy' is naturally resolved by a strongly anisotropic (truncated) Fermi surface [42], hosting separated charge and spin degrees of freedom. A generic starting point is the quantum spin-singlet liquid forming at the energy scale $T^\star$ — this spin-liquid groundstate is void of any long range order and competes with the antiferromagnet [45–47]. Upon doping, the spin-liquid becomes energetically favorable, charge and spin degrees of freedom separate and holes are expected to condense on the spin-liquid background, turning phase coherent at a lower energy T_c.

7 Concluding remarks

Hence, we conclude that at the edge of the pseudogap, a Zeeman scaling relation holds for both $H \| ab$ and $H \| c$. This implies that the pseudogap closing field H_{pg} arises from the correlations in the spin-channel that persist far into the strongly overdoped regime. The considerations above naturally lead to two field scales: the spin degrees are connected to the Zeeman field H_{pg} and the charge degrees are connected to the orbital field H_{c2}^N obtained through the Nernst transport. The *in-plane* Nernst transport reflects the dissipation due to nodal quasiparticles [25] in the vortex cores, with momenta nearly parallel to (π, π). Consequently, H_{c2}^N inhibits hole-pairing at the Fermi surface diagonals, but does not destroy the spin-singlet pairs around the Fermi surface corners – these spin-singlets are unpaired at the much higher Zeeman field H_{pg}. The breakup of the spin-singlets leaves its trace in the c-axis tunnelling experiment, since during the tunnelling process spin and charge degrees recombine into conventional carriers. Therefore, the identification of two limiting magnetic fields H_{c2}^N and H_{pg} deriving from the same pseudogap energy scale $T^\star$ via an orbital and a Zeeman relation, respectively, finds a natural interpretation in terms of a reconstructed Fermi surface with separated charge and spin degrees of freedom, arising in the scenarios for high-T_c based on a doped Mott insulator [45–47].

We wish to acknowledge our early collaboration with N. Morozov, L.N. Bulaevskii, M.P. Maley, Y.I. Latyshev, and T. Yamashita. We thank C.H. Mielke, B. Brandt, F.F. Balakirev, and J. Betts for technical assistance, M. Li and P.H. Kes for providing the underdoped crystals, T. Tamegai for the use of the crystal growth facilities, G. Blatter for his many insightful inputs, and A. Koshelev, V.M. Kogan, and M. Suzuki for their collegiality. Measurements were performed at NHMFL supported by the NSF Cooperative Agreement No. DMR-9527035. T.S. is supported by a Grant-in-Aid for Scientific Research from MEXT.

References

1. J. Orenstein, A. Millis, Science **288**, 468 (2000)
2. P.W. Anderson, Science **235**, 1196 (1987)
3. M.A. Kastner et al., Rev. Mod. Phys. **70**, 897 (1998)
4. L. Alff et al., Nature **422**, 698 (2003)
5. C. Bernhard et al., Phys. Rev. Lett. **86**, 1614 (2001)
6. V.J. Emery, S.A. Kivelson, Nature **374**, 434 (1995)
7. T. Timusk, B. Statt, Rep. Prog. Phys. **62**, 61 (1999) and references therein
8. M. Oda, N. Momono, M. Ido, Supercond. Sci. Technol. (UK) **13**, R139 (2000)
9. M.R. Norman et al., Nature **392**, 157 (1998)
10. Ch. Renner et al., Phys. Rev. Lett. **80**, 149 (1998)
11. M. Kugler et al., Phys. Rev. Lett. **86**, 4911 (2001)
12. Y. Yanase et al., Phys. Rep. **387**, 1 (2003)
13. Z.A. Xu et al., Nature **406**, 486 (2000)
14. V.M. Krasnov et al., Phys. Rev. Lett. **84**, 5860 (2000)
15. M. Suzuki, T. Watanabe, Phys. Rev. Lett. **85** 4787 (2000)
16. V.M. Krasnov et al., Phys. Rev. Lett. **86**, 2657 (2001)
17. J.L. Tallon, J.W. Loram, Physica C **349**, 53 (2001)
18. S. Chakravarty et al., Phys. Rev. B **63**, 094503 (2001)
19. C.M. Varma, Phys. Rev. Lett. **83**, 3538 (1999)
20. T. Shibauchi et al., Phys. Rev. Lett. **86**, 5763 (2001)
21. Y.-J. Kao et al., Phys. Rev. B **64**, R140505 (2001)
22. P. Pieri, G.C. Strinati, D. Moroni, Phys. Rev. Lett. **89**, 127003 (2002)
23. A.M. Clogston, Phys. Rev. Lett. **9**, 266 (1962)
24. N. Morozov et al., Phys. Rev. Lett. **84**, 1784 (2000)
25. L.B. Ioffe, A.J. Millis, Phys. Rev. B **58**, 11631 (1998)
26. T. Valla et al., Phys. Rev. Lett. **85**, 828 (2000)
27. T. Ito, K. Takenaga, S. Uchida, Phys. Rev. Lett. **70**, 3995 (1993)
28. T. Watanabe, T. Fujii, A. Matsuda, Phys. Rev. Lett. **84**, 5848 (2000)
29. K. Takenaka et al., Phys. Rev. B **50**, 6534 (1994)
30. M. Suzuki, T. Watanabe, A. Matsuda, Phys. Rev. Lett. **82**, 5361 (1999)
31. A.E. Koshelev, Phys. Rev. Lett. **76**, 1340 (1996)
32. J.-M. Triscone et al., Phys. Rev. B **50**, 1229 (1994)
33. G. Blatter et al., Rev. Mod. Phys. **66**, 1125 (1994)
34. Y. Ando et al., Phys. Rev. B **60**, 12475 (1999)
35. S.I. Vedeneev, Yu.N. Ovchinnikov, JETP Lett. **75**, 195 (2002)
36. L. Krusin-Elbaum, T. Shibauchi, C.H. Mielke, Phys. Rev. Lett. **92**, 097005 (2004)
37. Y.F. Yan et al., Phys. Rev. B **52**, R751 (1995)
38. A.N. Lavrov, Y. Ando, S. Ono, Europhys. Lett. **57**, 267 (2002)
39. T. Shibauchi et al., Phys. Rev. B **67**, 064514 (2003)
40. L.N. Bulaevskii et al., Phys. Rev. B **50**, 3507 (1994)
41. Y. Wang et al., Science **299**, 86 (2003); Y. Wang et al., Phys. Rev. Lett. **88**, 257003 (2002)
42. A. Damascelli, Z. Hussain, Z.-X. Shen, Rev. Mod. Phys. **75**, 473 (2003)
43. X.J. Zhou et al., Nature **423**, 398 (2003)
44. L. Krusin-Elbaum, G. Blatter, T. Shibauchi, Phys. Rev. B **69**, 220506 (2004)
45. P.W. Anderson, *The Theory of Superconductivity in the High-T_c Cuprate Superconductors* (Princeton University Press, Princeton, 1997)
46. Patrick A. Lee, Physica C **388-389**, 7 (2003)
47. C. Honerkamp, M. Salmhofer, T.M. Rice, Eur. Phys. J. B **27**, 127 (2002)